Deficiency for Costimulatory Receptor 4-1BB Protects Against Obesity-Induced Inflammation and Metabolic Disorders

Chu-Sook Kim,[1] Jae Geun Kim,[2] Byung-Ju Lee,[2] Myung-Sook Choi,[3] Hye-Sun Choi,[2] Teruo Kawada,[4] Ki-Up Lee,[5] and Rina Yu[1]

OBJECTIVE—Inflammation is an important factor in the development of insulin resistance, type 2 diabetes, and fatty liver disease. As a member of the tumor necrosis factor receptor superfamily (TNFRSF9) expressed on immune cells, 4-1BB/CD137 provides a bidirectional inflammatory signal through binding to its ligand 4-1BBL. Both 4-1BB and 4-1BBL have been shown to play an important role in the pathogenesis of various inflammatory diseases.

RESEARCH DESIGN AND METHODS—Eight-week-old male 4-1BB–deficient and wild-type (WT) mice were fed a high-fat diet (HFD) or a regular diet for 9 weeks.

RESULTS—We demonstrate that 4-1BB deficiency protects against HFD-induced obesity, glucose intolerance, and fatty liver disease. The 4-1BB–deficient mice fed an HFD showed less body weight gain, adiposity, adipose infiltration of macrophages/T cells, and tissue levels of inflammatory cytokines (e.g., TNF-α, interleukin-6, and monocyte chemoattractant protein-1 [MCP-1]) compared with HFD-fed control mice. HFD-induced glucose intolerance/insulin resistance and fatty liver were also markedly attenuated in the 4-1BB–deficient mice.

CONCLUSIONS—These findings suggest that 4-1BB and 4-1BBL may be useful therapeutic targets for combating obesity-induced inflammation and metabolic disorders. ***Diabetes*** **60:3159–3168, 2011**

Chronic inflammation is an important factor contributing to the development of various metabolic diseases, for example, type 2 diabetes, fatty liver, and atherosclerosis (1,2). Adipose tissue inflammation, a hallmark of obesity and type 2 diabetes, is closely associated with metabolic deregulation in liver and muscle and contributes to systemic inflammatory conditions (3). Adipose tissue produces various adipocytokines/chemokines, including tumor necrosis factor (TNF)-α, interleukin (IL)-6, and monocyte chemoattractant protein (MCP)-1, that induce inflammation. These inflammatory proteins cause insulin resistance by modulating insulin signaling and lipid metabolism (1,4). Recent studies emphasize the role of immune cells (e.g., macrophages/T cells) in adipose tissue in the development of metabolic diseases (5). In addition, depletion of $CD8^+$ T cells or $CD4^+$Th1 cells ameliorates systemic insulin resistance by lowering macrophage infiltration and inflammatory cytokines in the adipose tissue (6,7).

The inflammatory cascade is triggered by cross talk between T cells and macrophages, and interaction of cell surface receptors (e.g., antigen receptor and costimulatory receptors) with their counterpart ligands is involved in this cross talk (8). As a member of the TNF receptor superfamily (TNFRSF9) expressed on the cell surface, 4-1BB/CD137 provides a costimulatory signal through binding to its ligand 4-1BBL (CD137L/TNFRSF9). Although 4-1BB is expressed primarily on activated T cells and activated NK cells (9), 4-1BBL is expressed on a variety of antigen-presenting cells, including monocytes/macrophages, dendritic cells, activated B cells, and endothelial cells (10,11), and 4-1BB/4-1BBL signaling, which occurs bidirectionally, regulates various inflammatory events, such as immune cell survival, proliferation, cytokine production, and cytotoxicity (10,12). Moreover, modulation of 4-1BB/4-1BBL signaling has been shown to affect several inflammatory processes (e.g., asthma, colitis, rheumatoid arthritis, multiple sclerosis, type 1 diabetes, atherosclerosis, and cancer) in rodents (13–15) and is an attractive possibility for immune therapy of human cancers (16,17). The involvement of 4-1BB/4-1BBL signaling in metabolic diseases has not been established. However, given the accumulation of T cells and macrophages in obese adipose tissue, 4-1BB/4-1BBL may well have a role in obesity-induced adipose tissue inflammation and obesity-related metabolic disorders.

In this study, we demonstrate that 4-1BB deficiency reduces high-fat diet (HFD)–induced body weight gain and lowers glucose intolerance and fatty liver by reducing inflammatory responses. Hence, 4-1BB and 4-1BBL may be useful targets for treating obesity-induced inflammation and metabolic disorders.

RESEARCH DESIGN AND METHODS

Eight-week-old male 4-1BB–deficient mice on a C57BL/6 background, and their counterpart wild-type (WT) littermate controls, were bred and housed in a specific pathogen-free animal facility at the University of Ulsan. The 4-1BB–deficient mice on a C57BL/6 background were established in the University of Ulsan Immunomodulation Research Center (18). Homozygous 4-1BB–deficient mice ($4\text{-}1BB^{-/-}$) were bred with C57BL/6 mice for at least nine generations to obtain the 4-1BB–deficient mice on a C57BL/6 background. Genotypes of offspring were determined by Southern blot analysis of DNA obtained from tails. The mice were fed an HFD (60% of calories from fat; Research Diets Inc., New Brunswick, NJ) or a regular diet (RD; 13% calories from soybean oil; Harlan Teklad, Madison, WI) for 9 weeks and given food and water without restriction. Body weights were measured every week. All animal experiments

From the [1]Department of Food Science and Nutrition, University of Ulsan, Ulsan, South Korea; the [2]Department of Biological Science, University of Ulsan, Ulsan, South Korea; the [3]Department of Food Science and Nutrition, Kyungpook National University, Daegu, South Korea; the [4]Graduate School of Agriculture, Kyoto University, Uji, Kyoto, Japan; and the [5]Department of Internal Medicine, University of Ulsan College of Medicine, Seoul, South Korea.
Corresponding author: Rina Yu, rinayu@ulsan.ac.kr.
Received 30 December 2010 and accepted 9 September 2011.
DOI: 10.2337/db10-1805
This article contains Supplementary Data online at http://diabetes.diabetesjournals.org/lookup/suppl/doi:10.2337/db10-1805/-/DC1.
C.-S.K. and J.G.K. contributed equally to this work.

were approved by the animal ethics committee of the University of Ulsan and conformed to National Institutes of Health guidelines.

Glucose tolerance and insulin tolerance tests. Glucose tolerance tests were performed after a 5-h fast. Blood glucose concentrations were measured with a commercially available enzymatic assay kit (Asan Pharmacology, Hwa-Seong, Korea) before and 15, 30, 60, 90, and 120 min after oral administration of a 20% glucose solution at a dose of 2 g/kg. Insulin tolerance tests were carried out in animals that were fasted for 5 h. After an intraperitoneal bolus injection (0.75 units/kg) of recombinant human regular insulin (Human Regular; Eli Lilly, Indianapolis, IN), blood glucose concentrations were measured before and 20, 40, 60, 80, and 100 min after insulin injection.

Analysis of metabolic parameters. Mice were killed after a 4-h fast, and blood was collected by heart puncture. Plasma total cholesterol and triglyceride (TG) concentrations were determined using commercially available enzymatic assay kits (Asan Pharmacology). Plasma insulin levels were measured with an ultrasensitive mouse insulin ELISA kit (Mercodia, Uppsala, Sweden). Plasma high molecular weight (HMW) adiponectin levels were measured with an adiponectin HMW ELISA kit (ALPCO Immunoassays, Salem, NH). Hepatic TG content was assayed by saponification in ethanolic KOH, and glycerol content was measured with an FG0100 kit (Sigma-Aldrich, Saint Louis, MO) after neutralization with $MgCl_2$ (19). All tissue TG values were converted to glycerol content and corrected for liver weight.

Histochemistry. Adipose and liver tissues were fixed overnight at room temperature in 10% formaldehyde and embedded in paraffin. Tissues were sectioned (8-μm thick), stained with hematoxylin-eosin, and mounted on glass slides. Stained sections were viewed with an Axio-Star Plus microscope (Carl Zeiss, Gottingen, Germany). Adipocyte dimensions were measured using Axiovision AC software (Carl Zeiss) from images of hematoxylin-eosin stained cells.

Isolation of adipose tissue stromal vascular fraction leukocytes. To isolate adipose tissue–derived stromal vascular fractions (SVFs), fat pads from epididymal, renal, and mesenteric areas were minced and digested for 30 min at 37°C with type 2 collagenase (1 mg/mL; Sigma-Aldrich) in Dulbecco's modified Eagle's medium, pH 7.4. The suspensions were then passed through sterile 100-μm nylon meshes (SPL Lifesciences, Pocheon, Korea) and centrifuged at 500*g* for 10 min. They were resuspended in erythrocyte lysis buffer, incubated at room temperature for 3 min, and centrifuged at 500*g* for 5 min. Leukocytes were isolated from the SVFs on 40–70% Percoll gradients (GH Healthcare, Uppsala, Sweden). The tubes were centrifuged at 600*g* at room temperature for 30 min, and the leukocyte layers formed between the 40 and 70% layers of Percoll were retained.

Fluorescence-activated cell sorter analysis. Cells (5×10^5) isolated from adipose tissue were incubated with Fc-γ receptor–blocking antibodies (2.4G2) for 10 min on ice and double stained with phycoerythrin-conjugated anti-CD4, anti-CD8, or anti-CD11b antibody and fluorescein isothiocyanate–conjugated anti-CD4, anti-CD8, anti-CD44, anti-CD62L, or anti-F4/80 antibody. The cells were then washed with fluorescence-activated cell sorter (FACS) buffer and analyzed on a FACSCalibur (BD Biosciences, San Jose, CA) with CellQuest software (BD Biosciences).

Western blot analysis. Mice were fasted for 5 h, injected intraperitoneally with human insulin (10 mU/g body wt), and killed 4 min later. Skeletal muscle, liver, and adipose tissues were dissected and immediately frozen in liquid nitrogen. Next, samples of 20–50 μg total protein were subjected to Western blot analysis using polyclonal antibodies to phosphorylated Akt (Akt-pSer^{473}) and total Akt (Cell Signaling, Beverly, MA). Phosphorylation by AMP-activated protein kinase (AMPK) in the liver was detected using polyclonal antibodies to phosphorylated AMPK (AMPK-pThr^{172}) and total AMPK (Cell Signaling). Liver peroxisome proliferator–activated receptor (PPAR)-α was detected using mouse anti–PPAR-α antibody (Santa Cruz Biotechnology, Santa Cruz, CA).

Quantitative real-time PCR. Tissues were collected and stored at −20°C in RNAlater (Ambion, Austin, TX). Total RNA was extracted from tissues using TRIzol (Invitrogen, Carlsbad, CA), and cDNA was synthesized using M-MLV reverse transcriptase (Promega, Madison, WI). Real-time PCR amplification of the cDNA was performed in duplicate with a SYBR premix Ex Taq kit (TaKaRa Bio Inc., Forster, CA) using a Thermal Cycler Dice (TaKaRa Bio Inc., Shiga, Japan). All reactions were performed in the same manner: 95°C for 10s, 45 cycles of 95°C for 5s and 60°C for 30s. Details are listed in Supplementary Data online.

Measurement of cytokines. Adipose tissue samples (0.5 g) and liver samples (0.1 g) were homogenized with 1 mL 100 mmol/L Tris-HCl and 250 mmol/L sucrose buffer, pH 7.4, supplemented with protease inhibitors. Lipids were removed by centrifugation at 10,000*g*. The levels of TNF-α, MCP-1, IL-6, and adiponectin protein in the homogenates were measured with an OptEIA mouse TNF-α, MCP-1 set (BD Biosciences) and an IL-6 and adiponectin ELISA kit (R&D Systems, Minneapolis, MN). Amounts of cytokine were normalized for protein content, and the protein content of homogenates was determined with a BCA protein assay kit (Pierce, Rockford, IL).

Nuclear factor-κB activity. Nuclear factor-κB (NF-κB) DNA binding activity was assessed with a TransAM kit (Active Motif, Rixensart, Belgium). Samples of tissue homogenate normalized for protein content were incubated with immobilized oligonucleotides containing an NF-κB consensus binding site. DNA binding activity was analyzed with antibodies specific for the NF-κB subunits according to the manufacturer's instructions (Active Motif).

Indirect calorimetry. Energy expenditure was measured using an indirect calorimeter (Oxylet; Panlab, Cornella, Spain). The mice were acclimated in individual metabolic chambers, in which they had free access to food and water, and the O_2 and CO_2 analyzers were calibrated with highly purified gas. Oxygen consumption and carbon dioxide production were recorded at 3-min intervals using a computer-assisted data acquisition program (Chart 5.2; AD Instrument, Sydney, Australia) over a 24-h period, and the data were averaged for each mouse. Energy expenditure (EE) was calculated according to the following formula:

$$EE(kcal/day/body\,wt^{0.75}) = Vo_2 \times 1.44 \times [3.815 + (1.232 \times Vo_2/Vco_2)]$$

Body temperature and locomotor activity. Body temperature and locomotor activity were measured in WT and 4-1BB knockout (KO) mice using biotelemetry transmitters (Mini-Mitter, Bend, OR) implanted into the abdominal cavity 1 week before the experiment. Before surgery, mice were anesthetized with tribromoethanol (250 mg/kg body wt; Sigma-Aldrich). The output frequency in hertz was monitored by a receiver (model RA 1000; Mini-Mitter) placed under each cage. A data acquisition system (Vital View; Mini-Mitter) was used for automatic control of data collection and analysis. Body temperature was recorded at 10-min intervals and was summed after 24 h. Changes in locomotor activity were detected as changes in the position of the implanted transmitter over the receiver board, which resulted in changes of signal strength that were recorded as pulses of activity. These were counted every 10 min and were summed after 24 h.

Statistical analysis. Results are presented as means ± SEM. Statistical analyses were performed by Student *t* test or by ANOVA with Duncan multiple-range test. Differences were considered to be significant at $P < 0.05$.

RESULTS

HFD increases *4-1BB* and *4-1BBL* expression. To test whether expression of 4-1BB and/or its ligand 4-1BBL is altered by HFD-induced obesity, we measured levels of *4-1BB/4-1BBL* mRNAs in the adipose tissue and liver of mice fed an HFD or RD for 9 weeks. The levels of *4-1BB/4-1BBL* mRNAs in adipose tissue and liver were significantly higher in the HFD-fed mice than in the RD-fed mice (Fig. 1). In a similar manner, the plasma levels of soluble 4-1BBL in the HFD-fed mice were higher than in the RD-fed mice (Supplementary Fig. 1).

HFD-induced body weight gain and adiposity are reduced in 4-1BB–deficient mice. As expected, no *4-1BB* mRNA was detected in the adipose tissue, liver, and muscle of 4-1BB–deficient mice (Fig. 2*A*). The 4-1BB–deficient mice and WT controls were fed an RD or HFD for 9 weeks (Fig. 2*B*). The body weights of the 4-1BB–deficient mice given an HFD increased significantly less than that of the WT control mice, whereas there was no significant difference in body weight gain between WT control and 4-1BB–deficient mice fed an RD (Fig. 2*B*). Since total energy intake did not differ in the two HFD-fed groups (Fig. 2*C*), this suggests that HFD-fed 4-1BB–deficient mice dissipate more energy than HFD-fed WT mice.

While there was no difference in adiposity between the 4-1BB–deficient and WT mice fed an RD (Fig. 2*B–D*), the weights of the epididymal, renal, mesenteric, and subcutaneous fat pads in the HFD-fed 4-1BB–deficient mice were all significantly lower than those in the HFD-fed WT mice (Fig. 2*D*). The average area of adipocytes in the HFD-fed 4-1BB–deficient mice (3,690 ± 458 μm^2) was lower than that in the HFD-fed WT controls (5,826 ± 339 μm^2) (Fig. 2*E*), while adipocyte numbers did not differ between the two groups. There also was no difference between the two groups in the weights of other organs (liver, pancreas, muscle, and spleen) (data not shown).

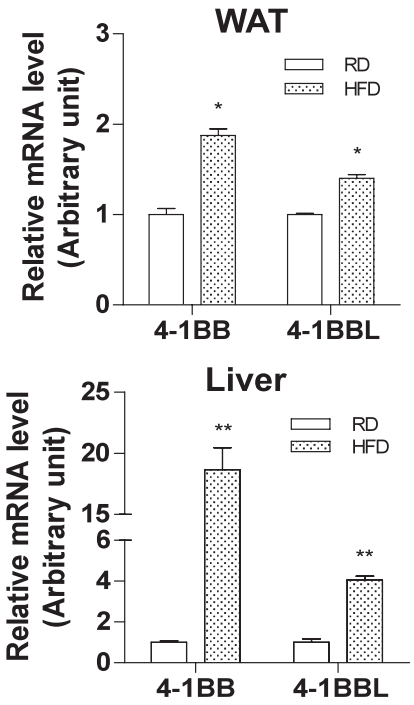

FIG. 1. HFD upregulates *4-1BB* and *4-1BBL* gene expression in adipose tissue and liver. C57BL/6 mice were fed an HFD or RD for 9 weeks. Levels of the mRNAs of *4-1BB* and *4-1BBL* in the epididymal adipose tissue (*upper*) and liver (*lower*) of mice fed an RD or HFD. Levels of mRNA were estimated by quantitative PCR. Results are means ± SEM (n = 4 mice per group). *$P < 0.05$, **$P < 0.01$ compared with RD. WAT, white adipose tissue.

Increased energy expenditure, locomotor activity, and hyperthermia in 4-1BB–deficient mice. To see whether the reduced body weight gain and adiposity observed in the 4-1BB–deficient mice fed an HFD was due to increased energy expenditure, we measured body temperature, locomotor activity, and energy expenditure. Body temperature and locomotor activity measured by the frequency of voluntary movements were higher in the HFD-fed 4-1BB–deficient mice than in the HFD-fed WT mice, as was energy expenditure during the dark phases (Fig. 3*A*–*C*). These differences were accompanied by upregulation of UCP-1 protein expression in brown adipose tissue (BAT) (Fig. 3*D*) and by smaller lipid droplets in the BAT of the HFD-fed 4-1BB–deficient mice (Fig. 3*E*). No significant differences were found between the two groups in plasma T3 and free T4 concentrations (data not shown). These findings suggest that 4-1BB deficiency increases energy expenditure.

Inflammatory cell infiltration and cytokine levels are lower in the adipose tissue of 4-1BB–deficient mice. To see whether 4-1BB deficiency affects obesity-induced adipose tissue inflammatory responses, we compared the infiltration of T cells and macrophages and cytokine levels in adipose tissue. Histochemical analysis showed that infiltration of cells into adipose tissue was lower in the HFD-fed 4-1BB–deficient mice than in the HFD-fed controls (Fig. 4*A*). Immunohistochemical analysis revealed that $CD3^+$ cells and crown-like structures representing aggregated $F4/80^+$ macrophages were less frequent in the adipose tissue of the HFD-fed 4-1BB–deficient mice than in that of the HFD-fed WT mice (Supplementary Fig. 2*A* and *B*). FACS analysis revealed that total numbers of T cells ($CD4^+$ or $CD8^+$), macrophages ($CD11b^+F4/80^+$), and activated T cells ($CD44^+/CD62L^-$) (Fig. 4*C*) were lower in the HFD-fed 4-1BB–deficient mice than in the HFD-fed controls. The percentage of T cell ($CD4^+$, $CD4^+/CD44^+/CD62L^-$) population, which is crucial for the infiltration and activation of macrophages, significantly decreased in the HFD-fed 4-1BB–deficient mice (Fig. 4*B*).

Reduced inflammatory cytokine levels in the 4-1BB–deficient mice. The 4-1BB–deficient mice given an HFD contained lower levels of inflammatory adipocytokine/chemokine proteins (TNF-α, IL-6, and MCP-1) in their adipose tissue than the HFD-fed WT obese mice (Fig. 5*A*), whereas there was no difference between these mice on an RD (data not shown). The levels of adiponectin in the epididymal adipose tissue were higher in the HFD-fed 4-1BB–deficient mice, although no difference was found in circulating plasma HMW/total adiponectin levels between HFD-fed 4-1BB–deficient mice and HFD-fed WT obese mice (Fig. 5*B*). Since the expression of the inflammatory genes for TNF-α and MCP-1 is regulated by the transcription factor NF-κB (20–22), we examined whether the 4-1BB signal affects the NF-κB pathway. As shown in Fig. 5*C*, DNA binding activity due to NF-κB subunit p65 in protein extracts of adipose nuclei was significantly lower in the HFD-fed 4-1BB–deficient mice.

Greater glucose tolerance/insulin sensitivity and insulin signaling in the 4-1BB–deficient mice. The fasting plasma glucose and insulin levels of the HFD-fed 4-1BB–deficient mice were significantly lower than those of the HFD-fed WT mice (Fig. 6*A*), whereas there was no difference on an RD (data not shown). Plasma TGs and total cholesterol levels were significantly lower (Fig. 6*B*). Oral glucose tolerance and insulin tolerance tests revealed that the HFD-fed 4-1BB–deficient mice were more glucose tolerant and more insulin sensitive than the HFD-fed WT mice (Fig. 6*C* and *D*). Insulin-stimulated glucose uptake was significantly higher in the isolated adipose tissue of HFD-fed 4-1BB–deficient mice than in that of the HFD-fed WT mice (Supplementary Fig. 3*A*), and this was associated with increased levels of insulin receptor substrate 1 (*IRS1*) and *GLUT4* mRNAs (Supplementary Fig. 3*B*). Akt phosphorylation was also significantly higher in the muscle, adipose tissue, and the liver of the 4-1BB–deficient obese mice (Fig. 6*E*), suggesting that insulin signaling is more efficient.

Fat accumulation, metabolic responses, and liver inflammation. We next examined whether 4-1BB deficiency influenced HFD-induced fatty liver. Liver tissue collected after 9 weeks of HFD revealed that the livers of the 4-1BB–deficient mice were darker than those of the WT mice, and histological analysis revealed less fat accumulation in the former (Fig. 7*A*). Hepatic TGs were also twofold lower in the HFD-fed 4-1BB–deficient mice (Fig. 7*B*). Since this could be attributable to either reduced TG synthesis or increased hepatic fatty acid oxidation, we examined the expression of lipogenic genes (e.g., *SREBP-1c*, *ACC1*, and *FAS*) and found that it was significantly lower in the livers of the HFD-fed 4-1BB–deficient mice (Fig. 7*C*). Western blots showed that phosphorylated AMPK and PPAR-α were elevated, and acetyl-CoA carboxylase was lower in the livers of the HFD-fed 4-1BB–deficient mice (Fig. 7*D*), suggesting increased fatty acid oxidation in these mice. In addition, levels of inflammatory cytokines (i.e., TNF-α and IL-6) were reduced in the livers of the HFD-fed 4-1BB–deficient mice (Fig. 7*E*), and the MCP-1 level tended to decrease (Fig. 7*E*).

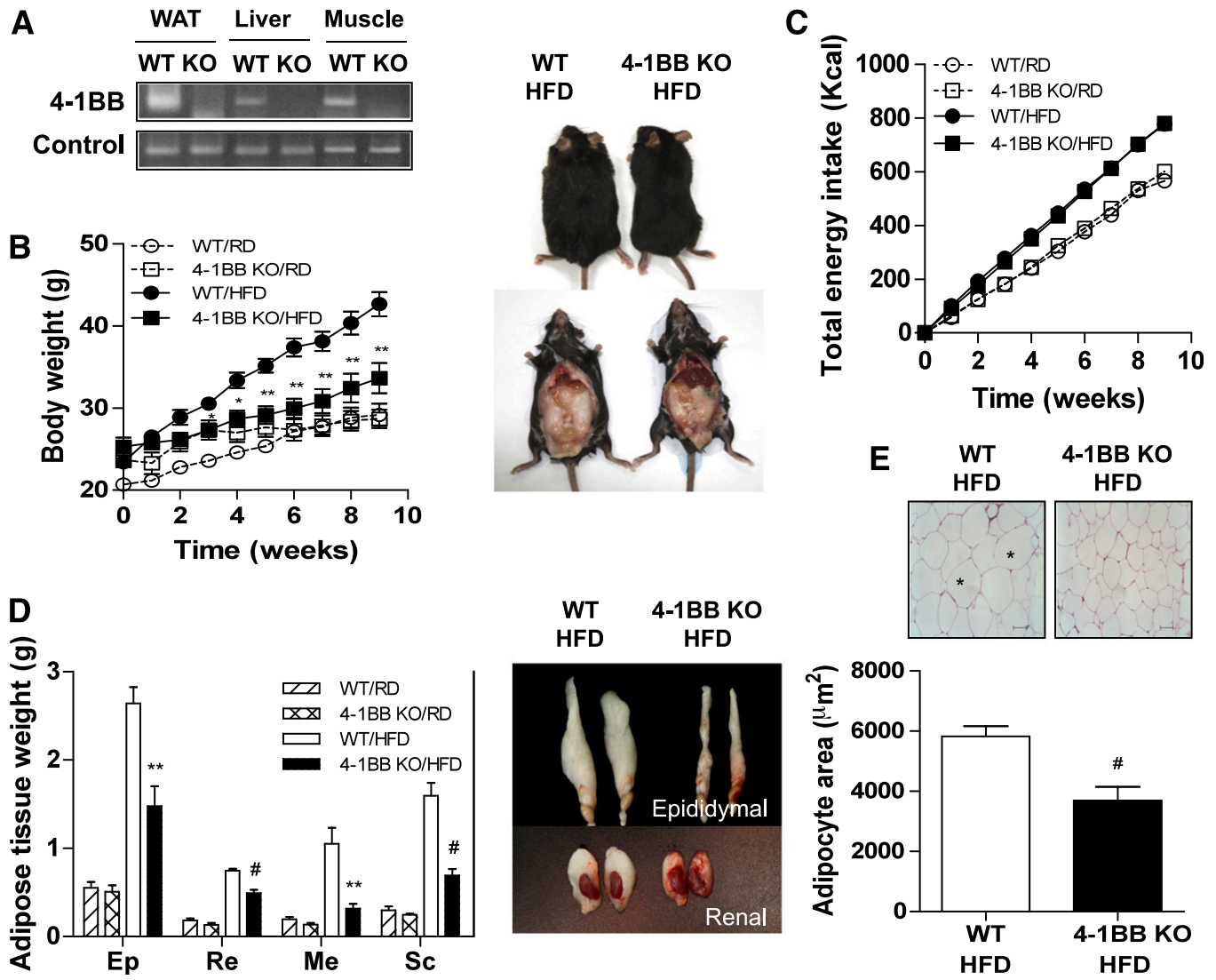

FIG. 2. Body weight change and adiposity in HFD-fed 4-1BB–deficient mice. WT and 4-1BB–deficient mice were fed an HFD for 9 weeks. *A*: Expression of *4-1BB* mRNA in epididymal adipose tissue, liver, and skeletal muscle. Body weight changes and gross morphology of mice (*B*), energy intake (*C*), and adipose tissue weight (Ep, epididymal; Re, retroperitoneal; Me, mesenteric; and Sc, subcutaneous) of WT (n = 8) and 4-1BB–deficient mice (n = 8) fed an RD or HFD, and gross morphology of adipose tissues (*D*). Results are means ± SEM. *P < 0.05, **P < 0.01, #P < 0.005 compared with WT mice fed an HFD. *E*: Histological analysis of epididymal adipose tissue and size distribution of adipocytes from WT and 4-1BB–deficient mice fed an HFD. Sections were stained with hematoxylin-eosin. Hypertrophied adipocytes are indicated by asterisks. Original magnification is ×200 (scale bar = 50 μm). The sizes of adipocytes in randomly chosen fields were measured with a microscope (magnification ×200) and calculated using Axiovision AC software. #P < 0.005 compared with WT mice fed an HFD. WAT, white adipose tissue. (A high-quality color representation of this figure is available in the online issue.)

DISCUSSION

In this study, we show that 4-1BB deficiency reduces HFD-induced weight gain, glucose intolerance, fatty liver disease, and lowered adipose tissue inflammatory responses. In control mice, HFD markedly increased *4-1BB* and/or *4-1BBL* gene expression in adipose tissues and liver as well as plasma soluble 4-1BBL levels, suggesting possible participation of these molecules in adipose and whole body inflammatory responses.

Using 4-1BB–deficient mice fed an HFD, we found that the infiltration of macrophages and T cells ($CD4^+$, $CD8^+$, and activated T cells) into adipose tissue was markedly decreased in the HFD-fed 4-1BB–deficient mice. Adipose T-cell infiltration has been shown to precede macrophage infiltration (23), and activated T cells are considered to regulate adipose tissue inflammation by modulating macrophage infiltration and altering their inflammatory phenotype (23,24). Accordingly, the decreased adipose T-cell infiltration/activation in the 4-1BB–deficient obese mice may limit the accumulation of macrophages, and inflammatory responses, in the adipose tissue. A previous study shows that the failure to develop herpetic stromal keratitis in 4-1BB–deficient mice is associated with reduced T-cell migration into the corneal stroma (25). It was also recently reported that 4-1BB is expressed on blood vessel walls at sites of inflammation and enhances monocyte migration (26). Taken together, these findings suggest that limiting T-cell/macrophage infiltration into inflamed adipose tissue in obesity by blocking 4-1BB signaling could be a useful therapeutic strategy against obesity-related inflammation.

Persistent cell/cell cross-talk between immune cells (antigen-presenting cells and T cells) and nonimmune cells through cell surface molecules stimulates inflammatory cytokine release and leads to chronic inflammation

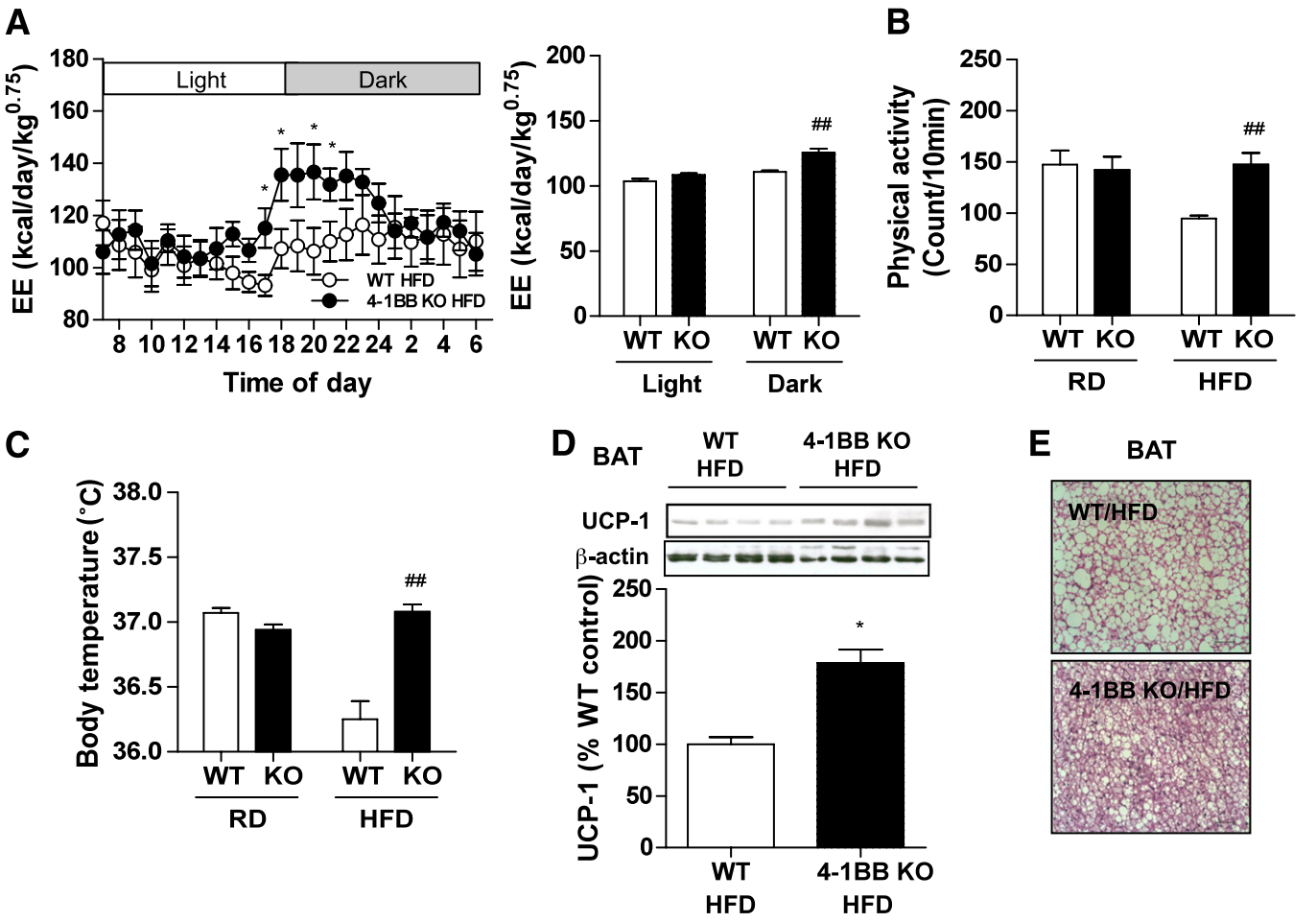

FIG. 3. Energy expenditure, locomotor activity, and body temperature in 4-1BB–deficient mice. *A*: Energy expenditure (EE) was measured in WT (n = 4) and 4-1BB–deficient mice (n = 4) fed an HFD. Locomotor activity (*B*) and body temperature (*C*) were measured in WT (n = 10–11) and 4-1BB–deficient mice (n = 7) fed an RD or HFD. Results are means ± SEM. *P < 0.05, ##P < 0.001 compared with WT mice fed an HFD. *D*: Levels of UCP-1 protein in BAT. Levels of protein were determined by Western blotting. The intensities of UCP-1 protein were normalized to those of β-actin and are expressed as means ± SEM of 4 mice per group. *P < 0.05 compared with WT mice fed an HFD. *E*: Histological analysis of BAT from WT and 4-1BB–deficient mice fed an HFD (hematoxylin-eosin). Original magnification is ×200 (scale bar = 50 μm). (A high-quality color representation of this figure is available in the online issue.)

(11,27,28). For example, 4-1BB is functionally expressed on endothelial cells, and the interaction between endothelial cell 4-1BB and monocyte 4-1BBL promotes vascular inflammation by inducing monocyte migration and cytokine production (11,27). In this context, it may be proposed that 4-1BB/4-1BBL participates in adipose tissue inflammatory responses by promoting interaction between adipose cells and infiltrated T cells/macrophages and that disruption of 4-1BB may reduce these responses. Indeed, HFD-fed 4-1BB–deficient mice had lower levels of inflammatory adipocytokines/chemokines (e.g., TNF-α, IL-6, and MCP-1) and increased levels of the anti-inflammatory adipocytokine adiponectin than HFD-fed WT controls.

It is noteworthy that expression of both 4-1BB and 4-1BBL in adipose tissue and liver increased in mice fed an HFD. *MCP-1* expression was significantly decreased in the macrophages, adipocytes, and/or hepatocytes of the HFD-fed 4-1BB–deficient mice (Supplementary Fig. 4), suggesting that this decrease may reduce macrophage infiltration. Of interest, in addition to the 4-1BB–mediated inflammatory signals, reverse signaling through 4-1BBL in monocytes/macrophages promotes the secretion of proinflammatory cytokines (29,30). Since bidirectional signaling occurs (26,31) and *4-1BBL* is expressed on hepatic macrophage Kupffer cells (Supplementary Fig. 5), the absence of the 4-1BB/4-1BBL interaction in 4-1BB–deficient mice may prevent macrophages or T cells from being activated in the liver and/or adipose tissue. Bone marrow transplantation experiments would be desirable to clarify the mechanisms by which the 4-1BB–deficient mice are protected from HFD-induced inflammation and metabolic disorders.

The 4-1BB signaling pathway is associated with activation of NF-κB signaling (32), whereas reverse signaling by 4-1BBL is mediated by protein tyrosine kinases (e.g., p38 mitogen-activated protein kinase; extracellular signal–regulated kinases 1, 2; mitogen-activated protein/extracellular signal–regulated kinase; and phosphoinositide-3-kinase) (30). In the current study, we found that NF-κB activation was markedly decreased in the adipose tissue of the HFD-fed 4-1BB–deficient mice. This suggests that 4-1BB–mediated inflammatory signaling, presumably involved in the cross talk between T cells and macrophages, or between immune cells and nonimmune cells such as adipocytes or hepatocytes, may be blunted in 4-1BB–deficient adipose tissue and/or liver, with a resulting reduction in inflammatory responses.

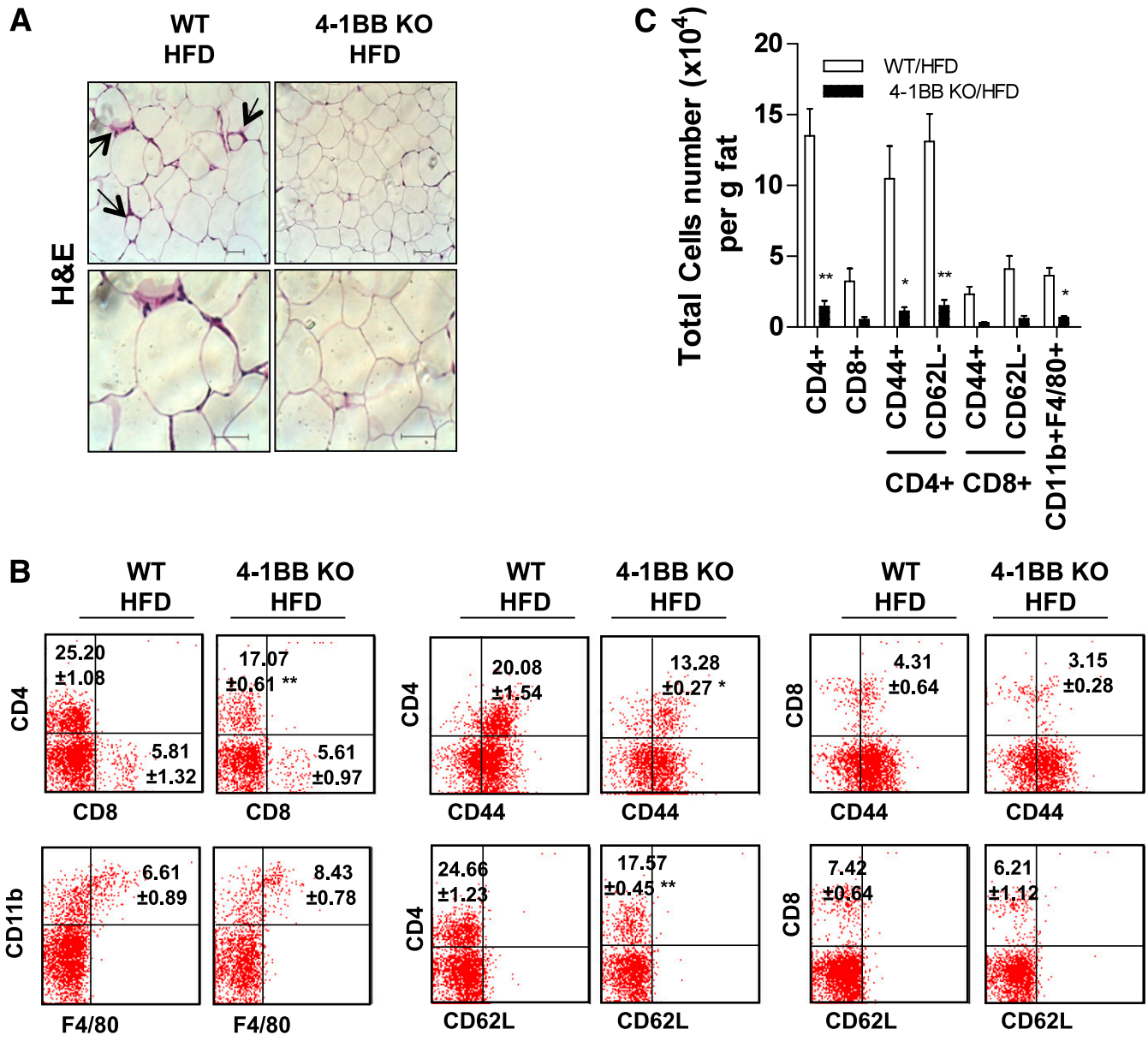

FIG. 4. Adipose tissue macrophages and T cells in HFD-fed 4-1BB–deficient mice. *A*: Histological analysis of epididymal adipose tissue from WT and 4-1BB–deficient mice fed an HFD. Sections were stained with hematoxylin-eosin (H&E) in epididymal adipose tissue from WT and 4-1BB–deficient mice fed an HFD. Stained cells are indicated by arrows. Original magnifications are ×200 (*upper*) and ×400 (*lower*) (scale bar = 50 μm). FACS quantification of immune cell population and numbers in visceral adipose SVF from WT and 4-1BB–deficient mice fed an HFD. SVFs were double stained with fluorescein isothiocyanate–conjugated phycoerythrin-conjugated anti-CD4 (helper T cell)/anti-CD8 (cytotoxic T cell), anti-F4/80/CD11b (macrophage), anti-CD4 (or CD8)/CD44^{high} (activated T cell), and anti-CD4 (or CD8)/CD62L^{low} (activated T cell). *B*: The values in the panels indicate the percentages of each cell population. *C*: The total immune cell numbers in adipose tissue. Results are mean ± SEM. *$P < 0.05$, **$P < 0.01$ compared with WT mice fed an HFD. (A high-quality color representation of this figure is available in the online issue.)

Obesity-induced inflammation is closely associated with the development of insulin resistance and type 2 diabetes. Inflammatory cytokines can cause insulin resistance by modulating insulin signaling and lipid metabolism (1,4). Moreover, depletion of $CD8^+$ T cells or $CD4^+$Th1 cells ameliorates systemic insulin resistance by reducing macrophage infiltration and inflammatory cytokine levels in adipose tissue (6,7). Thus, the improved glucose tolerance in the HFD-fed 4-1BB–deficient mice could be the result of lower numbers of $CD4^+$ and $CD8^+$ T cells and macrophages in the adipose tissue, leading to reduced inflammatory cytokine levels. In our study, adiponectin expression was increased in the adipose tissue of the HFD-fed 4-1BB–deficient mice, and this also may have contributed to the sensitization of insulin responsiveness in the mice (33,34).

Recent studies show that accumulation of TG in the liver and skeletal muscle results in insulin resistance by inhibiting the insulin receptor signaling cascades (35,36). In the HFD-fed 4-1BB–deficient mice, TG accumulation in liver and skeletal muscle was significantly reduced (data not shown). This may be due to decreased lipid synthesis and/or increased lipid oxidation, leading to reduced hepatic steatosis and plasma TG levels. Reduced levels of expression of lipogenic genes (*SREBP-1c*, *ACC1*, and *FAS*) and increased expression of PPAR-α and AMPK

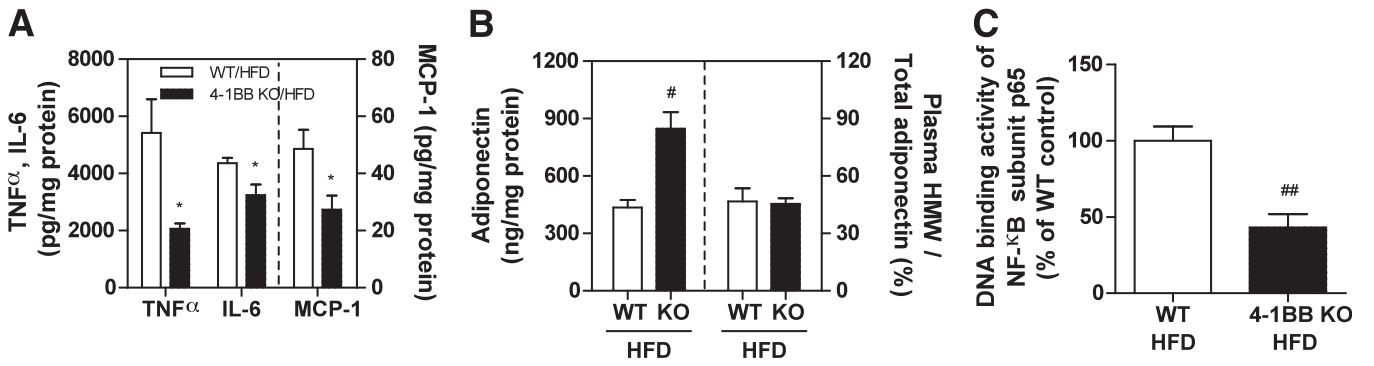

FIG. 5. Adipose tissue inflammatory responses in HFD-fed 4-1BB–deficient mice. Concentrations of inflammatory proteins (TNF-α, IL-6, and MCP-1) (*A*) and an anti-inflammatory protein (adiponectin) (*B*) in adipose tissue from WT (n = 8) and 4-1BB–deficient mice (n = 8) fed an HFD. Adipose tissue (0.5 g) was homogenized with 1 mL of 100 mmol/L Tris-HCl and 250 mmol/L sucrose buffer (pH 7.4) supplemented with protease inhibitors. Lipids were removed by centrifugation at 10,000*g* for 10 min. Levels of cytokines/adipokines in homogenates were measured by enzyme-linked immunosorbent assay and normalized for protein content. Levels of HMW adiponectin were assessed in plasma samples from WT (n = 8) and 4-1BB–deficient mice (n = 8). Results are mean ± SEM. *P < 0.05, #P < 0.005 compared with WT mice fed an HFD. *C*: NF-κB activation in adipose tissue was determined using the p65 TransAM assay as described in RESEARCH DESIGN AND METHODS. Results are mean ± SEM (n = 6 mice per group). ##P < 0.001 compared with WT mice fed an HFD.

phosphorylation in the liver (37,38) suggest that 4-1BB has a regulatory role in lipid metabolism that merits further exploration.

Another intriguing aspect of our results is the finding that 4-1BB deficiency results in reduced body weight gain and adiposity in obese mice fed an HFD. Despite the reduction of adiposity, no difference was observed between the dietary intake of the HFD-fed 4-1BB–deficient mice and HFD-fed controls. Moreover, the reduced physical activity and body temperature observed in HFD-fed mice were

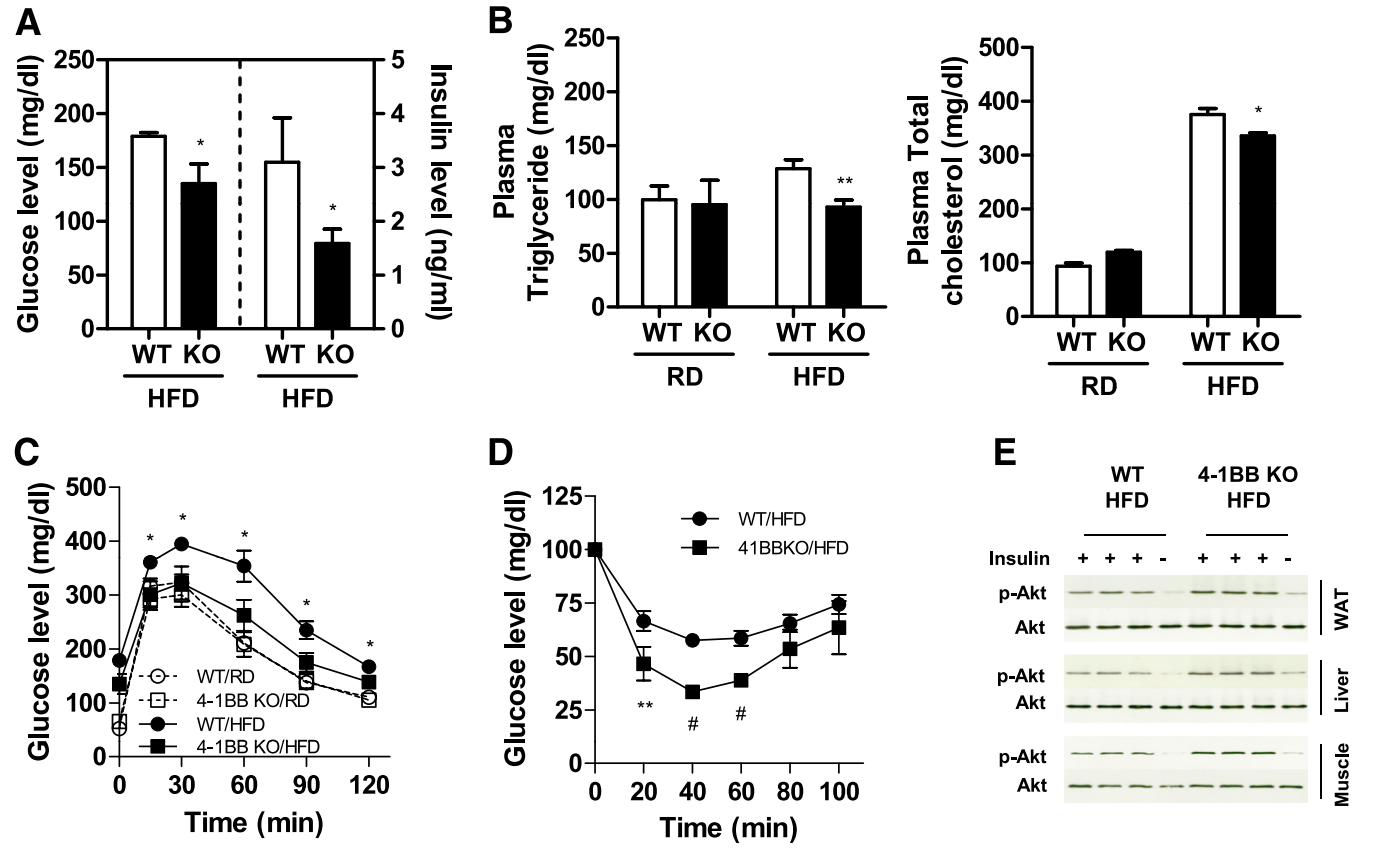

FIG. 6. Deficiency of 4-1BB ameliorates insulin resistance and improves insulin signaling in mice fed an HFD. *A*: Fasting glucose and insulin levels. *B*: Plasma TG and total cholesterol levels in WT and 4-1BB–deficient mice fed an RD or HFD. Results are means ± SEM (n = 5–6 mice per group). *P < 0.05, **P < 0.01 compared with WT mice fed an HFD. *C*: Glucose tolerance tests. Mice fed an HFD for 7 weeks were fasted for 5 h before receiving an oral administration of 20% glucose solution at a dose of 2 g/kg, and blood samples were taken at the indicated times (n = 5). *D*: Insulin tolerance tests. Mice fed an HFD for 7 weeks were fasted for 5 h before receiving an intraperitoneal injection of 0.75 units/kg insulin, and blood samples were taken at the indicated times (n = 5). Results are means ± SEM. *P < 0.05, **P < 0.01, #P < 0.005 compared with WT mice fed an HFD. *E*: Western blots of phosphorylated Akt (p-Akt) and total Akt in adipose tissue, liver, and skeletal muscle from WT (n = 4) and 4-1BB–deficient mice (n = 4) fed an HFD. Mice were fasted for 5 h before receiving a 10 mU/g i.p. insulin injection and killed 4 min later, and tissues were collected for Western blotting. WAT, white adipose tissue. (A high-quality color representation of this figure is available in the online issue.)

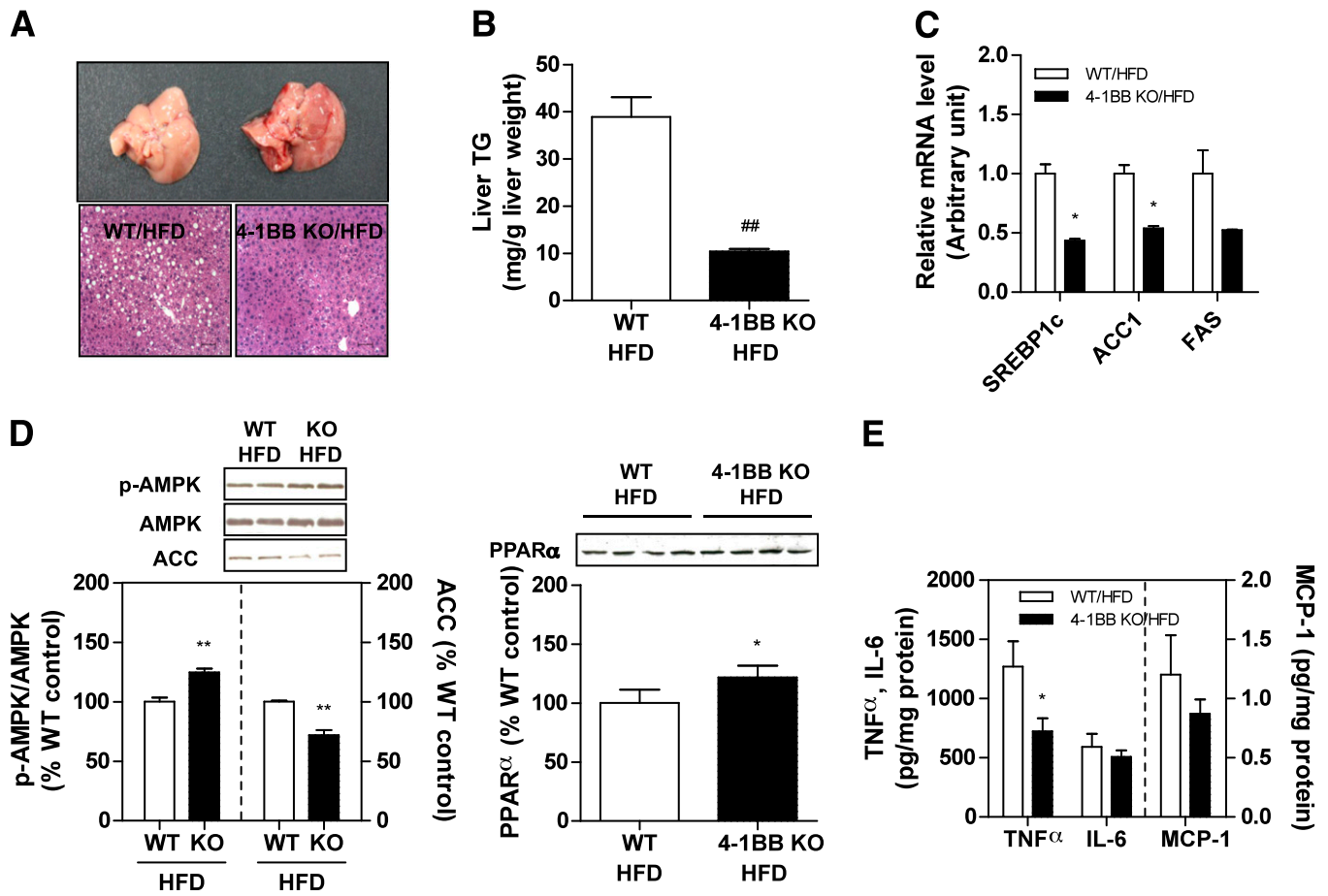

FIG. 7. Deficiency of 4-1BB ameliorates hepatic steatosis. *A*: Gross morphology and histological analysis (hematoxylin-eosin) of livers from WT and 4-1BB–deficient mice fed an HFD. Original magnification is ×200 (scale bar = 50 μm). *B*: Levels of TG content of livers from WT (n = 4) and 4-1BB–deficient mice (n = 4) fed an HFD. Results are means ± SEM. ##P < 0.001 compared with WT mice fed an HFD. *C*: Expression of lipogenic genes (*SREBP-1*, *ACC1*, and *FAS*) in livers from WT (n = 4) and 4-1BB–deficient mice (n = 4) fed an HFD. Levels of mRNA were estimated by quantitative PCR. Results are means ± SEM. *P < 0.05 compared with WT mice fed an HFD. *D*: Western blots of phosphorylated AMPK (p-AMPK), acetyl-CoA carboxylase (ACC), and PPAR-α in livers from WT and 4-1BB–deficient mice fed an HFD. The intensity of the bands was quantified by densitometry and is expressed as means ± SEM (n = 4 mice per group). **P < 0.05 compared with WT mice fed an HFD. *E*: Levels of inflammatory proteins (TNF-α, IL-6, and MCP-1) in livers from WT (n = 8) and 4-1BB–deficient mice (n = 8) fed an HFD. Levels of cytokines/chemokines in liver were measured by enzyme-linked immunosorbent assay. Results are means ± SEM. *P < 0.05, **P < 0.01 compared with WT mice fed an HFD. (A high-quality color representation of this figure is available in the online issue.)

restored to normal in the 4-1BB–deficient mice, indicating that 4-1BB is somehow involved in the reduced physical activity and body temperature of HFD mice. Given that the inflammatory cytokine TNF-α inhibits UCP-1 expression in BAT (39), the increased UCP-1 protein level in the BAT of HFD-fed 4-1BB–deficient mice suggests that the reduced severity of inflammation in HFD-fed 4-1BB–deficient mice may be linked to the restoration of body temperature. Alternatively, since 4-1BB is expressed in brain cells, including neurons, astrocytes, and microglial cells (40,41) it is possible that the thermogenic response observed in HFD-fed 4-1BB–deficient mice is, at least in part, mediated via the central nervous system.

It should be noted that disruption of several inflammatory receptors (e.g., TNFR1, Toll-like receptors, and IL-1R) enhances thermogenesis and fat oxidation and improves insulin resistance in mice fed an HFD (42–44). The disruption of various inflammatory signaling molecules (e.g., inhibitor of κB kinase, Jun NH_2-terminal kinase, and NF-κB) also affects adiposity and lipid/glucose metabolism (45–47). Given that inflammatory signaling molecules are associated with 4-1BB/4-1BBL signaling, it is tempting to speculate that 4-1BB/4-1BBL–mediated signals may share or interact with metabolic signals required for inflammatory cellular responses. The absence of 4-1BB/4-1BBL signaling presumably enhances catabolic/thermogenic pathways, which contributes to protection from obesity. The mechanism by which 4-1BB/4-1BBL elicit their effects on metabolic signaling remain to be defined.

A number of studies show that targeting the interaction between 4-1BB/4-1BBL suppresses mouse models of inflammatory diseases (e.g., rheumatoid arthritis, atherosclerosis, and experimental autoimmune myocarditis) (14,15,27). In addition, 4-1BB is considered an attractive target for immunotherapy of many immune/inflammatory diseases in humans. These results suggest that blocking 4-1BB/4-1BBL as a form of immunobiological therapy may be effective in reducing inflammation-associated obesity and metabolic diseases. However, in view of the controversy surrounding the therapeutic effect of neutralizing TNF-α antibody on insulin resistance in obese and type 2 diabetic subjects (48–50), the efficacy of blocking 4-1BB in human metabolic disease needs to be established. Moreover, since 4-1BB–deficient mice display reduced humoral and cell-mediated

immunity accompanied by altered myeloid progenitor cell growth (18), the potential deleterious effects of 4-1BB–related intervention should be carefully considered prior to its therapeutic application. Further studies are needed to establish the therapeutic potential of 4-1BB/4-1BBL blockade in controlling human obesity and metabolic diseases.

In conclusion, our data demonstrate that 4-1BB deficiency reduces HFD-induced adiposity, inflammatory responses, glucose intolerance, and fatty liver disease. Preventing 4-1BB and 4-1BBL cross talk may reduce obesity-induced inflammation and metabolic disorders, such as insulin resistance and fatty liver disease. Both 4-1BB and 4-1BBL may be useful therapeutic targets against obesity-induced inflammation and metabolic disorders.

ACKNOWLEDGMENTS

This work was supported by the Midcareer Researcher Program through National Research Foundation (NRF) Grant KOSEF 2009-0079485 funded by the Ministry of Education, Science, and Technology (MEST) and the 2009 Research Fund of University of Ulsan. In addition, the study was partially supported by the Science Research Center program (Center for Food & Nutritional Genomics Grant 2010-0001886) of the NRF of Korea funded by the MEST. T.K. was supported by the Grants-in-Aid for Scientific Research from the Ministry of Education, Culture, Sport, Science, and Technology of Japan (22228001).

No potential conflicts of interest relevant to this article were reported.

C.-S.K. researched data and wrote the manuscript. J.G.K. researched data and contributed to discussion. B.-J.L., M.-S.C., H.-S.C., and T.K. contributed to discussion. K.-U.L. contributed to discussion and reviewed and edited the manuscript. R.Y. researched data, contributed to discussion, and wrote, reviewed, and edited the manuscript.

REFERENCES

1. Hotamisligil GS, Shargill NS, Spiegelman BM. Adipose expression of tumor necrosis factor-alpha: direct role in obesity-linked insulin resistance. Science 1993;259:87–91
2. Shoelson SE, Lee J, Goldfine AB. Inflammation and insulin resistance. J Clin Invest 2006;116:1793–1801
3. Hotamisligil GS. Inflammation and metabolic disorders. Nature 2006;444:860–867
4. Guilherme A, Virbasius JV, Puri V, Czech MP. Adipocyte dysfunctions linking obesity to insulin resistance and type 2 diabetes. Nat Rev Mol Cell Biol 2008;9:367–377
5. Weisberg SP, McCann D, Desai M, Rosenbaum M, Leibel RL, Ferrante AW Jr. Obesity is associated with macrophage accumulation in adipose tissue. J Clin Invest 2003;112:1796–1808
6. Nishimura S, Manabe I, Nagasaki M, et al. CD8+ effector T cells contribute to macrophage recruitment and adipose tissue inflammation in obesity. Nat Med 2009;15:914–920
7. Winer S, Chan Y, Paltser G, et al. Normalization of obesity-associated insulin resistance through immunotherapy. Nat Med 2009;15:921–929
8. Croft M. Co-stimulatory members of the TNFR family: keys to effective T-cell immunity? Nat Rev Immunol 2003;3:609–620
9. Hurtado JC, Kim SH, Pollok KE, Lee ZH, Kwon BS. Potential role of 4-1BB in T cell activation. Comparison with the costimulatory molecule CD28. J Immunol 1995;155:3360–3367
10. Vinay DS, Kwon BS. Role of 4-1BB in immune responses. Semin Immunol 1998;10:481–489
11. Olofsson PS, Söderström LA, Wågsäter D, et al. CD137 is expressed in human atherosclerosis and promotes development of plaque inflammation in hypercholesterolemic mice. Circulation 2008;117:1292–1301
12. Takahashi C, Mittler RS, Vella AT. Cutting edge: 4-1BB is a bona fide CD8 T cell survival signal. J Immunol 1999;162:5037–5040
13. Cheung CT, Deisher TA, Luo H, et al. Neutralizing anti-4-1BBL treatment improves cardiac function in viral myocarditis. Lab Invest 2007;87:651–661
14. Seo SK, Choi JH, Kim YH, et al. 4-1BB-mediated immunotherapy of rheumatoid arthritis. Nat Med 2004;10:1088–1094
15. Jeon HJ, Choi JH, Jung IH, et al. CD137 (4-1BB) deficiency reduces atherosclerosis in hyperlipidemic mice. Circulation 2010;121:1124–1133
16. Hernandez-Chacon JA, Li Y, Wu RC, et al. Costimulation through the CD137/4-1BB pathway protects human melanoma tumor-infiltrating lymphocytes from activation-induced cell death and enhances antitumor effector function. J Immunother 2011;34:236–250
17. Meseck M, Huang T, Ma G, Wang G, Chen SH, Woo SL. A functional recombinant human 4-1BB ligand for immune costimulatory therapy of cancer. J Immunother 2011;34:175–182
18. Kwon BS, Hurtado JC, Lee ZH, et al. Immune responses in 4-1BB (CD137)-deficient mice. J Immunol 2002;168:5483–5490
19. Salmon AG, Nash JA, Walklin CM, Freedman RB. Dechlorination of halocarbons by microsomes and vesicular reconstituted cytochrome P-450 systems under reductive conditions. Br J Ind Med 1985;42:305–311
20. Chen LW, Egan L, Li ZW, Greten FR, Kagnoff MF, Karin M. The two faces of IKK and NF-kappaB inhibition: prevention of systemic inflammation but increased local injury following intestinal ischemia-reperfusion. Nat Med 2003;9:575–581
21. Baeuerle PA, Baltimore D. NF-kappa B: ten years after. Cell 1996;87:13–20
22. Oberbach A, Schlichting N, Blüher M, et al. Palmitate induced IL-6 and MCP-1 expression in human bladder smooth muscle cells provides a link between diabetes and urinary tract infections. PLoS ONE 2010;5:e10882
23. Kintscher U, Hartge M, Hess K, et al. T-lymphocyte infiltration in visceral adipose tissue: a primary event in adipose tissue inflammation and the development of obesity-mediated insulin resistance. Arterioscler Thromb Vasc Biol 2008;28:1304–1310
24. Strissel KJ, DeFuria J, Shaul ME, Bennett G, Greenberg AS, Obin MS. T-cell recruitment and Th1 polarization in adipose tissue during diet-induced obesity in C57BL/6 mice. Obesity (Silver Spring) 2010;18:1918–1925
25. Seo SK, Park HY, Choi JH, et al. Blocking 4-1BB/4-1BB ligand interactions prevents herpetic stromal keratitis. J Immunol 2003;171:576–583
26. Drenkard D, Becke FM, Langstein J, et al. CD137 is expressed on blood vessel walls at sites of inflammation and enhances monocyte migratory activity. FASEB J 2007;21:456–463
27. Haga T, Suzuki JI, Kosuge H, et al. Attenuation of experimental autoimmune myocarditis by blocking T cell activation through 4-1BB pathway. J Mol Cell Cardiol 2009;46:719–727
28. Fiocchi C. Intestinal inflammation: a complex interplay of immune and nonimmune cell interactions. Am J Physiol 1997;273:G769–G775
29. Schwarz H. Biological activities of reverse signal transduction through CD137 ligand. J Leukoc Biol 2005;77:281–286
30. Söllner L, Shaqireen D O Kwajah MM, Wu JT, Schwarz H. Signal transduction mechanisms of CD137 ligand in human monocytes. Cell Signal 2007;19:1899–1908
31. Shuford WW, Klussman K, Tritchler DD, et al. 4-1BB costimulatory signals preferentially induce CD8+ T cell proliferation and lead to the amplification in vivo of cytotoxic T cell responses. J Exp Med 1997;186:47–55
32. Croft M. The role of TNF superfamily members in T-cell function and diseases. Nat Rev Immunol 2009;9:271–285
33. Maeda N, Shimomura I, Kishida K, et al. Diet-induced insulin resistance in mice lacking adiponectin/ACRP30. Nat Med 2002;8:731–737
34. Fruebis J, Tsao TS, Javorschi S, et al. Proteolytic cleavage product of 30-kDa adipocyte complement-related protein increases fatty acid oxidation in muscle and causes weight loss in mice. Proc Natl Acad Sci USA 2001;98:2005–2010
35. Shulman GI. Cellular mechanisms of insulin resistance. J Clin Invest 2000;106:171–176
36. Petersen KF, Befroy D, Dufour S, et al. Mitochondrial dysfunction in the elderly: possible role in insulin resistance. Science 2003;300:1140–1142
37. Lee WJ, Kim M, Park HS, et al. AMPK activation increases fatty acid oxidation in skeletal muscle by activating PPARalpha and PGC-1. Biochem Biophys Res Commun 2006;340:291–295
38. Le May C, Pineau T, Bigot K, Kohl C, Girard J, Pégorier JP. Reduced hepatic fatty acid oxidation in fasting PPARalpha null mice is due to impaired mitochondrial hydroxymethylglutaryl-CoA synthase gene expression. FEBS Lett 2000;475:163–166
39. Valladares A, Roncero C, Benito M, Porras A. TNF-alpha inhibits UCP-1 expression in brown adipocytes via ERKs. Opposite effect of p38MAPK. FEBS Lett 2001;493:6–11
40. Lim HY, Kim KK, Zhou FC, Yoon JW, Hill JM, Kwon BS. 4-1BB-like molecule is expressed in islet-infiltrating mononuclear cells and in the gray matter of the brain. Cell Biol Int 2002;26:271–278

41. Reali C, Curto M, Sogos V, et al. Expression of CD137 and its ligand in human neurons, astrocytes, and microglia: modulation by FGF-2. J Neurosci Res 2003;74:67–73
42. Romanatto T, Roman EA, Arruda AP, et al. Deletion of tumor necrosis factor-alpha receptor 1 (TNFR1) protects against diet-induced obesity by means of increased thermogenesis. J Biol Chem 2009;284:36213–36222
43. Davis JE, Gabler NK, Walker-Daniels J, Spurlock ME. Tlr-4 deficiency selectively protects against obesity induced by diets high in saturated fat. Obesity (Silver Spring) 2008;16:1248–1255
44. Ehses JA, Meier DT, Wueest S, et al. Toll-like receptor 2-deficient mice are protected from insulin resistance and beta cell dysfunction induced by a high-fat diet. Diabetologia 2010;53:1795–1806
45. Chiang SH, Bazuine M, Lumeng CN, et al. The protein kinase IKKepsilon regulates energy balance in obese mice. Cell 2009;138:961–975
46. Hirosumi J, Tuncman G, Chang L, et al. A central role for JNK in obesity and insulin resistance. Nature 2002;420:333–336
47. Tang T, Zhang J, Yin J, et al. Uncoupling of inflammation and insulin resistance by NF-kappaB in transgenic mice through elevated energy expenditure. J Biol Chem 2010;285:4637–4644
48. Ofei F, Hurel S, Newkirk J, Sopwith M, Taylor R. Effects of an engineered human anti-TNF-alpha antibody (CDP571) on insulin sensitivity and glycemic control in patients with NIDDM. Diabetes 1996;45:881–885
49. Paquot N, Castillo MJ, Lefèbvre PJ, Scheen AJ. No increased insulin sensitivity after a single intravenous administration of a recombinant human tumor necrosis factor receptor: Fc fusion protein in obese insulin-resistant patients. J Clin Endocrinol Metab 2000;85:1316–1319
50. Huvers FC, Popa C, Netea MG, van den Hoogen FH, Tack CJ. Improved insulin sensitivity by anti-TNFalpha antibody treatment in patients with rheumatic diseases. Ann Rheum Dis 2007;66:558–559